Chemical Physics 559 (2022) 111541

Contents lists available at ScienceDirect

Chemical Physics

journal homepage: www.elsevier.com/locate/chemphys

Raman investigations and *ab initio* calculations of natural diamond-lonsdaleite originating from New Caledonia

Yassine El Mendili [a,b,*], Beate Orberger [c], Daniel Chateigner [b], Jean-François Bardeau [d], Stéphanie Gascoin [b], Sébastien Petit [b]

[a] COMUE Normandie Université – Laboratoire ESITC - ESITC Caen, 1 Rue Pierre et Marie Curie, 14610 Epron, France
[b] CRISMAT-ENSICAEN, UMR CNRS 6508, Normandie Université, 6 boulevard Maréchal Juin, 14050 Caen, France
[c] GEOPS-Paris Sud, Université Paris-Sud, UMR 8148 (CNRS-UPS), Bât 504, 91405 Orsay, France
[d] IMMM, Le Mans Université, UMR 6283 CNRS, Avenue Olivier Messiaen, 72085 Le Mans, France

ARTICLE INFO

Keywords:
Ab initio calculation
Lonsdaleite
Micro-Raman spectroscopy
Vibrational properties
Elastic properties
Electronic band structure

ABSTRACT

Here, we report the first occurrence so far of cubic diamond and lonsdaleite in a siliceous breccia hosted in nickel laterite from the Tiébaghi mine, New Caledonia. Diamond and lonsdaleite polytype occurred as minerals in surficial formed siliceous rocks. The vibrational properties and the calculated elastic properties and electronic band structure of 3C-diamond and lonsdaleite were studied by micro-Raman spectroscopy and *ab initio* calculation. Our measured Raman spectra demonstrate the coexistence of cubic diamond and lonsdaleite based on the correlation between *ab initio* calculation and experimental results. We showed that the position of the single Raman vibration mode for cubic diamond corresponds to the first order scattering of F_{2g} symmetry at 1332 cm^{-1}. For lonsdaleite, the *ab initio* calculations predict three fundamental vibrational modes: 1207 cm^{-1} (E_{2g}), 1307 cm^{-1} (A_{1g}), and 1330 cm^{-1} (E_{1g}). The calculated indirect bandgaps of 3C-diamond and lonsdaleite at room temperature are 5.7 eV and 5.2 eV, respectively. The elastic anisotropy calculations show that lonsdaleite has the greatest shear modulus, bulk modulus and young's modulus compared to cubic diamond, which indicates a high degree of hardness of this hexagonal structure of diamond.

1. Introduction

A series of diamond polytype structures are described and predicted [1–5]. Diamond polytypes are analogue to the widely known polytypes of SiC [3,5]. The intermediate orthorhombic diamond polytype was recently assessed using density-functional theory and formed by compressing graphite in the [0 0 1] direction at a pressure of 59.4 GPa [6]. In addition, end member polytypes of 3C and 2H diamonds have been previously established, and polytypes such as 4H, 6H and 8H diamonds are predicted, but not synthetized.

In its natural state, carbon exists in three crystalline forms: hexagonal graphite, cubic diamond, which is the most abundant crystalline form of diamond and known for its exceptional hardness (Moh's scale 10); and lonsdaleite, a very rare native form of carbon. Lonsdaleite was discovered in 1967 in meteorites from the famous Meteor Crater, Arizona [1,2]. The extreme heat and pressure of the impact are proposed having transformed graphite into diamond while retaining graphite's hexagonal crystal lattice. The hexagonal structure of lonsdaleite has also received much attention due to its superior mechanical properties, such as hardness, rigidity, and compressive strength. Indeed, lonsdaleite is simulated to be 58% harder than diamond on the ⟨1 0 0⟩ face and to withstand indentation pressures of 152 GPa, while diamond would break at 97 GPa [7]. This is yet exceeded by IIa diamond's ⟨1 1 1⟩ tip hardness of 162 GPa. Even the mechanical properties of londsdaleite suggest being superior to those of cubic diamond, it was never proved. High pressure (>130 kbar) high temperature (1000 °C) experiments could produce lonsdaleite as impurities in diamond [8]. Poorly crystalline lonsdaleite synthesis was achieved from C-rich fluids in association with graphite at 500 °C and 1000 atm [9]. According to Németh et al. is not possible to synthetize well crystallized lonsdaleite [10]. In nature, lonsdaleite is often associated with meteorite impacts, or in diamond placer deposits in the Sakha Republic, Northeastern Siberia [11,12]. The finding of lonsdaleite in sediments from Younger Dryas Boundary (YBD) was used as high evidence for supporting the "impact -model". However, the presence of these hexagonal diamond form at the YDB is highly questioned and disapproved [13,14]. Other authors

* Corresponding author at: COMUE Normandie Université – Laboratoire ESITC - ESITC Caen, 1 Rue Pierre et Marie Curie, 14610 Epron, France.
E-mail address: yassine.el-mendili@esitc-caen.fr (Y. El Mendili).

https://doi.org/10.1016/j.chemphys.2022.111541
Received 6 December 2021; Received in revised form 29 March 2022; Accepted 6 April 2022
Available online 9 April 2022

question the existence of lonsdaleite in general [10]. However, shock compression experiments on graphite by Kraus et al. [15] showed that lonsdaleite form at above 170 GPa. Lonsdaleite associated with graphite is also described from metasomatized gneiss in Kokchetav, Russia, a major diamond deposit [16].

Compared to graphite formed at low pressure, diamond is considered as a metastable form of carbon. The graphite structure was formed by a two-layer stacking sequence (ABABAB) of planar hexagonal (0 0 0 1) planes of carbon atoms, whereas diamond was made by three-layer stacking sequences (ABCABCABC) of the identical hexagonal but puckered (1 1 1) carbon atomic planes.

Graphite is made up of layers (x-y planes) with carbon atoms bonded together by sigma bonds. Each carbon atom in this layer is linked to three other carbon atoms, resulting in sp2 hybridized orbitals and trigonal planar geometry. Cubic diamond (3C-diamond) and lonsdaleite (2H-diamond) are composed of sp3 hybridized, meaning that each carbon atom is bonded to four other carbon atoms. These results in the tetrahedral structure with covalent and extremely strong bonds (sharing electrons) are shown in Fig. 1. Both 3C and 2H diamonds have puckered layers of carbon atoms with six-membered rings arranged in an armchair configuration.

The distinction between 3C and 2H diamonds, lies in how these layers are stacked on top of one another to form the three-dimensional crystal structure (Fig. 1). Identical layers are stacked on top of each other in 3C-diamond, with a shift halfway across the diagonal of a six-membered ring. Each layer in a 2H-diamond, on the other hand, is a mirror image of the previous layer [17]. The structural effect of these various stacking combination is that the six-membered rings connecting the different layers are armchair in 3C-diamond but boat-type in lonsdaleite. As a result, 3C-diamond is made up entirely of armchair rings, whereas lonsdaleite is made up of a 50:50 mix of armchair and boat rings.

Lonsdaleite was proposed to exhibit a wurtzite-type structure, belonging to the space group $P63/mmc$ and lattice parameters $a = 0.25$ and $c = 0.412$ nm [18–20]. These papers deal with lonsdaleite associated with 3C diamonds and moissanite in pores of a siliceous rocks which host saprolite fragments from the base of the nickel laterite profile at the Tiébaghi mine, New Caledonia [21]. This finding indicates that the siliceous rocks were formed later than the laterite soil. The nickel laterite soils have been formed on serpentinized peridotite, a Mg-Fe-Si rich rock which presents the upper earth mantle. The diamonds were investigated by El Mendili et al. [21,22]. The authors suggest that these diamonds were inherited from the saprolitized (weathered) serpentinized- peridotites. These diamonds may have formed in the lower earth mantle at high pressure, then being transported into the upper earth mantle by high temperature Mg-rich second stage melts (boninites), or were formed by low temperature hydrothermal alteration, the serpenitization process [23]. To decide on the ultimate origin of diamond and associated phases, an in-depth study on the serpentinized peridotites must be performed. This was beyond of this study.

The objective of this study was to perform ab-initio calculations to obtain the Raman spectra of different diamond polytypes. These calculations univocally evidence the presence of lonsdaleite.

2. Materials and methods

2.1. Materials

The diamond-lonsdaleite studied here, naturally occur in a siliceous rock (SB; SOLSA label: ER-NC00-0001) at the Tiébaghi mine in New Caledonia. The siliceous rock is porous of beige color. This rock hosts dark gray-brown fragments of saprolite. Saprolite is a weathered part of peridotite formed under reducing conditions at the base of the laterite profile. The siliceous rock locally shows reddish spots indicating local presence of ironoxihydroxides. The siliceous rocks cut through the saprolite horizon. It was formed after lateritization through weathering. For the origin of the diamonds and associated minerals the ultimate origin cannot be defined. So far, we can conclude that the diamonds and other reducing phases were inherited from the weathered and serpentinzed peridotites. They have survived hydrothermal (serpentinization) and weathering (atmospheric) conditions. Diamond microcrystals were inherited from the upper earth mantle [22].

Prior to the discussion of diamond and associated highly reducing phases occurring in the pores of the siliceous rock, we argue against that these phases are not artefacts produced as a result of diamond sawing during sample preparation: (i) the sample was prepared with three other rocks (sandstone, harzburgite, and granite), all of which were sawn with the same diamond blade [24]. (ii) micro-Raman spectroscopy was used to analyze all these samples [24,25], although only the siliceous breccia contains SiC-diamond polymorphs. (iii) diamond-lonsdaleite intergrowth is unlikely to be a characteristic of diamond saw generated particles. (iv) Clusters of diamond, chromite, and SiC polymorph are found in nature [26–28].

Possible contamination (diamond, SiC and corundum) of natural samples and methods for preventing sample contamination are discussed in recent literature [29–31]. Taking this into account, the sample preparation was carried out carefully.

2.2. Analytical methods

2.2.1. Scanning electron microscopy

Imaging, mapping and compositional analysis were performed using scanning electron microscope equipped with energy dispersive spectrometer (SUPRA™ 55Vp, Carl Zeiss Jena, Germany). The measurements were performed at 20 kV.

2.2.2. Raman spectroscopy

The Raman spectra were acquired using a DXR Raman microscope (Thermo Fisher Scientific, Inc., USA) fitted with a 900 lines/mm diffracting grating. Green excitation produced the highest signal-to-noise ratio (532 nm, Nd:YAG laser). Raman measurements were performed at a very low laser power (about 1mW at the sample surface) to avoid

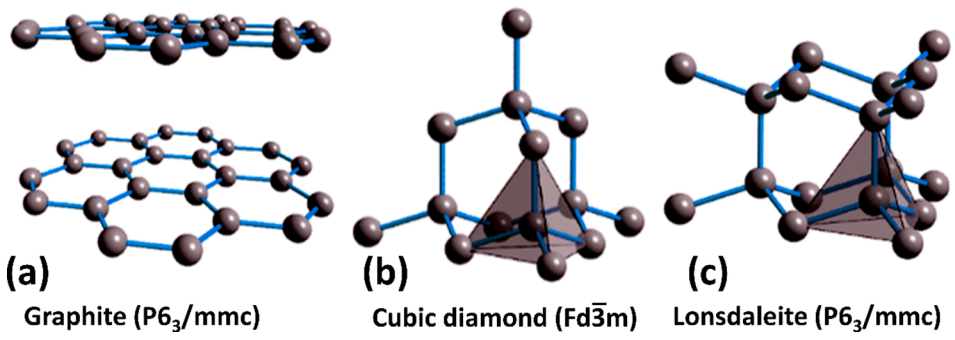

Fig. 1. Crystal structures of a) Graphite, b) Cubic diamond, and c) Lonsdaleite.

unintended heating, structural changes, or phase transitions. A 100× magnification long working distance objective (NA. 0.9) is selected to target the laser beam at the sample with a spot size evaluated to 0.6 μm and to collect the scattered light with spatial resolution of about 3 cm^{-1}. The raw data was obtained over an 80–2200 cm^{-1} range. Raman spectra were carefully recorded twice with a 120-seconds integration time. For each phase, three spectra were recorded and averaged. The peak deconvolution and integration were performed with the Origin software using the Gaussian function.

2.3. Calculation

The vibrational spectra of diamonds (3C and 2H) were investigated using the Crystal17 code based on first-principles density functional theory (DFT) [32]. CRYSTAL is an *ab initio* code that uses a Gaussian-type basis set to express crystalline orbitals (Bloch functions) [33]. For the truncation of Coulomb and lattice exchange series, the two different pseudo-overlap thresholds are used. A Monkhorst-Pack 16 × 16 × 16 grid appears well converged for cubic diamond and a Monkhorst-Pack 16 × 16 × 10 grid appears well converged for lonsdaleite. Wavenumbers at the Γ point are obtained within the Quasi-Harmonic Approximation (QHA) implemented in Crystal17 [34,35]. The relative intensities of Raman active modes were computed using a fully analytical approach by exploiting the scheme described by Maschio et al. [36–39]. The calculated Raman spectra of 3C and 2H diamond was drawn using a Lorentzian form with a FWHM of 3 and 10 cm^{-1}, respectively. Before calculating the elastic constants, the structures of diamond polytypes were fully relaxed until the atomic forces were less than 0.002 eV/Å. The density of states and the band structure of lonsdaleite were computed along high-symmetry line segments in the irreducible Brillouin zone.

3. Results and discussion

3.1. Structural properties of diamond polytypes

The porosities of siliceous rock were observed by optical microscopy (Fig. 2a). These porosities host small crystals shining several colors from blue to white colorless (Fig. 2a). Interestingly, spanning the Raman microscope beam inside the porosities revealed the presence of micrometric size diamonds arranged as clusters in most of the porosities of breccia samples (Fig. 2b). We separated some grains from these porosities, as clusters of several individual nano to micro-diamond crystallites, loosely bound to the surface of the samples. EDS analyzes confirm that these diamonds clusters do not contain elements heavier than carbon (Fig. 2d). It is important to note that some extracted grains with a light blue color and the largest dimension smaller than 65 μm was analyzed by single crystal X-ray diffraction (SCXRD) experiments [21]. SCXRD experiments were not successful in determining diamond spots with quantitative intensity resolution due to a micrometric size of diamonds crystals, which are arranged as clusters of several microcrystalites. Nevertheless, the presence of a twin law corresponding to a three-fold axis parallel to **c** has been observed by SCXRD.

3.2. Vibrational properties of diamond

Considering various structures of sp^3-carbon atoms, a series of superhard carbon allotropes is predicted, described, and investigated [40–50]. Two of them are observed in nature, 3C- diamond and 2H-diamond [8]. The Raman spectra of the diamonds investigated here exhibit a strong, first order peak of sp^3-bonded carbon located between 1331,4 and 1328 cm^{-1} (Fig. 3a, b, c), with Full Width at Half Maximum (FWHM) varying between 4.9 and 7.3 cm^{-1}. Since no additional vibrational mode was identified in the range of 60–4000 cm^{-1}, only the 1100–1500 cm^{-1} range is depicted. In addition, no graphite was found in our samples. The well-crystallized 3C-diamond has quite a peak at 1332 cm^{-1} with a FWHM of 3 cm^{-1}, while the 2H polymorph,

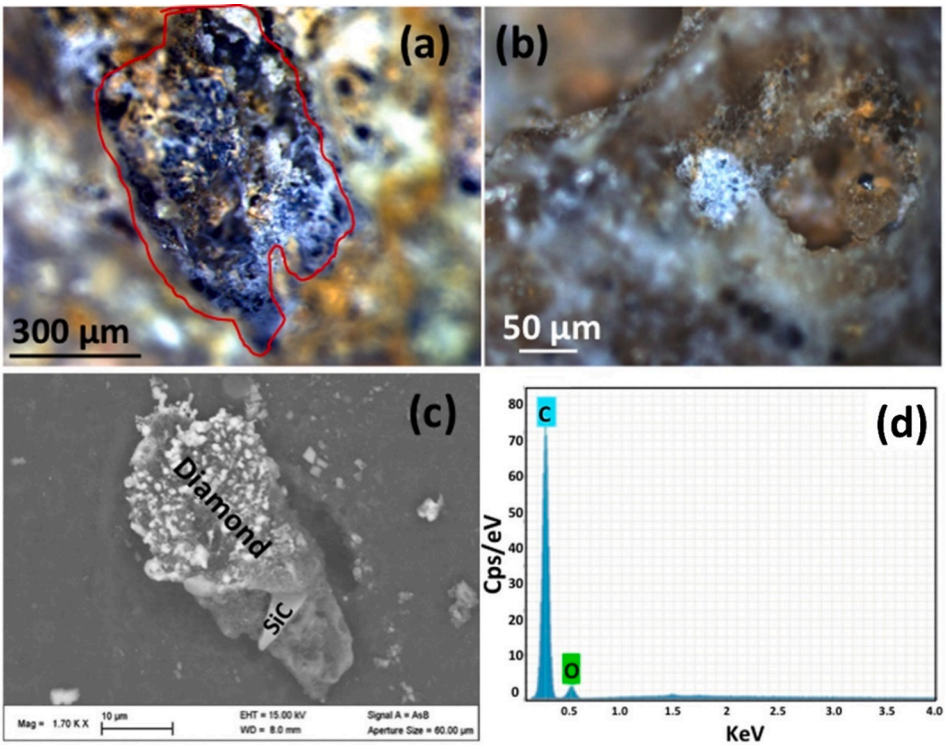

Fig. 2. Porosities of siliceous rock a) Binocular images of siliceous rock porosities, b) Optical images of diamond present in porosities, c) SEM image of a cluster of diamonds bearing SiC extracted from porosities and d) EDS spectrum of diamond.

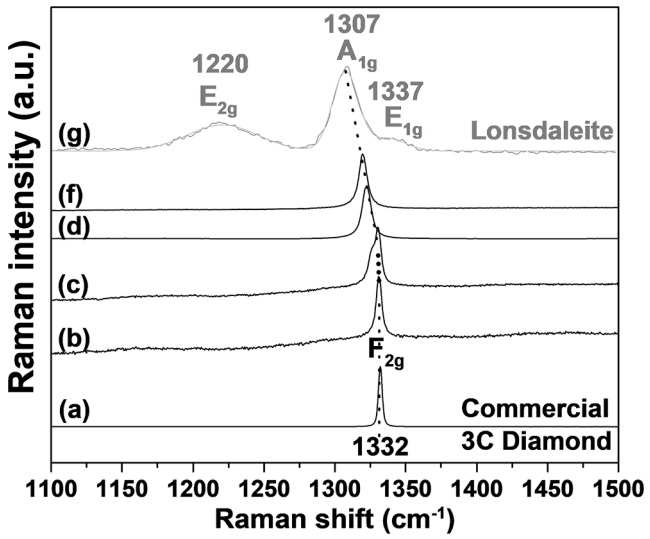

Fig. 3. Raman spectra of diamonds obtained from different breccia porosities. (a) Commercial well-crystallized cubic diamond, (b) Cubic diamond, (c) Diamond exhibiting two overlapped bands was recorded. The first at 1330.5 cm^{-1} and the second at 1326 cm^{-1}, (d) Diamond exhibiting Raman band at 1326 cm^{-1} (f) Diamond exhibiting Raman band at 1318 cm^{-1} and (g) Lonsdaleite.

lonsdaleite, has a fluctuating sp^3 breathing vibration mode between 1320 and 1327 cm^{-1} [43].

A commercial cubic diamond present in our sample exhibits a sp3 mode centered at 1332.0 ± 0.5 cm^{-1} with a FWHM of 4.9 ± 0.1 cm^{-1} (Fig. 3b). The slightly larger FWHM and low-frequency shift of the band may be induced by lower crystallinity (nano-sized) of the natural cubic diamond [48,51,52] as well as the heat of the sample (this effect was described in Supplementary materials of [53]), the last was control in our experiment with low power of exiting laser beam. Additionally, the contribution of lonsdaleite in Raman spectrum of lonsdaleite-diamond mixture (natural or synthetic samples) can lead to shift of total wide Raman band from 1332 cm^{-1} to lower value (up to 1320 cm^{-1} [38,47,49]).

A Raman spectrum with two overlapping bands (Fig. 3,c) was observed. The first, at 1330.5 ± 0.2 cm^{-1} corresponds to cubic symmetry, while the second, at 1326.2 ± 0.2 cm^{-1}, corresponds to hexagonal diamond. Individual crystals were not discernible under the microscope. These two contributions are due to the presence of nanometric cubic-hexagonal diamonds inclusions.

The sp^3 modes of the spectra (Fig. 3) in the 1320–1327 cm^{-1} region can be attributed to hexagonal diamond polytypes. Indeed, Smith and Godard [43] previously identified the lonsdaleite contribution in Raman spectra of impact diamond-bearing rocks exhibiting the strongest band about 1320–1327 cm^{-1}. X-ray diffraction revealed the existence of lonsdaleite in their samples.

Finally, spectra with sp^3 modes at values below 1320 cm^{-1} (Fig. 3f), were also observed before. Nishitani-Gamo et al. [45] suggested that this shift is due to stacking faults within the diamond structure, leading to the cubic-hexagonal transition. Finally, Fig. 3g shows a Raman spectrum with three Raman-active vibrational modes around 1220, 1307 and 1337 cm^{-1}. This spectrum is similar to those reported for lonsdaleite [46]. Even though the theoretical calculations of the vibrational spectrum of lonsdaleite have been the focus of many studies over the years, various uncertainties and contradictions about the vibrational attribution and the band position remain [46,47,54]. As a result, Density Functional Theory was used to compute the Raman-active vibrational modes of 3C and 2H diamonds. We performed these calculations at the Γ point using harmonic approximation, as it was by Goryainov *et al.* have done [47] for Raman identification of lonsdaleite. For cubic diamond the position of the single Raman vibrational band, corresponding to the first order scattering of F_{2g} symmetry, is 1332 cm^{-1} (Fig. 4). This value agrees well with the experimental value. DFT predicts three basic vibrational modes for lonsdaleite: E_{2g}: 1207 cm^{-1}, A_{1g}: 1307 cm^{-1}, and E_{1g}: 1330 cm^{-1} with a theoretical intensity ratio of 1(A_{1g}):0.5(E_{2g}):0.3 (E_{1g}).

According to the comparison of theoretical and measured Raman spectrum (Figs. 3 and 4), the intense vibrational mode observed in the experimental Raman spectrum at 1307 cm^{-1} with a FWHM of 18 cm^{-1} is obviously assigned to the longitudinal optical vibrational mode A_{1g}. The shoulder band identified as a transverse optical vibrational mode (E_{2g}) of lonsdaleite detected at 1220 cm^{-1} with a FWHM of 37 cm^{-1} (Table 1).

This correlates to the *ab initio* computations. Indeed, DFT simulations also suggest that the third Raman-active mode of lonsdaleite assigned to E_{1g} transverse optical will be observed at 1337 cm^{-1} with a FWHM of 18 cm^{-1} and an intensity comparable to that of the E_{1g} mode (Fig. 4). When compared to the cubic diamond observed in the porosities of siliceous breccia (ER-NC00-0001), the lonsdaleite bands are widely broadened (FWHM between 18 and 52 cm^{-1}). This phenomenon is caused by lonsdaleite imperfections and tiny crystallite dimensions.

3.3. Elastic properties of diamond

The calculated and experimental elastic constant tensors for 3C-diamond and lonsdaleite crystals are listed in Table 2 along with available computed and experimental elastic constants. The bulk modulus (B) is computed using the second order tensor.

For cubic crystals, tensor C_{ij} has three typical and independent elastic constants (C_{11}, C_{12}, and C_{44}), which define the mechanical hardness and are necessary for specifying the stability of the material.

According to Born structural stability, the elastic constants satisfy the conditions C_{11}-$C_{12} > 0$, $C_{11} > 0$, $C_{11} + 2C_{12} > 0$ [57]. As another result, the present C_{11}, C_{12}, and C_{44} values well confirm both the structural and cubic stability conditions for diamond.

For hexagonal crystals, tensor C_{ij} has six nonzero elastic constants, five of which (C_{11}, C_{12}, C_{13}, C_{33}, and C_{44}) are independent and the sixth (C_{66}) is determined by the relation $C_{66} = (C_{11} - C_{12})/2$ [57]. The elastic constants determine the stability of hexagonal crystal structure when the following conditions are satisfied [56]: $C_{44} > 0$, $C_{11} > C_{12}$, and $(C_{11} + 2C_{12})\,C_{44} > 2C_{13}^2$. These inequalities are valid for lonsdaleite.

The elastic anisotropy calculations show that the lonsdaleite has the greatest shear modulus, bulk modulus and Young's modulus compared to cubic diamond. This is the indication of high hardness of this

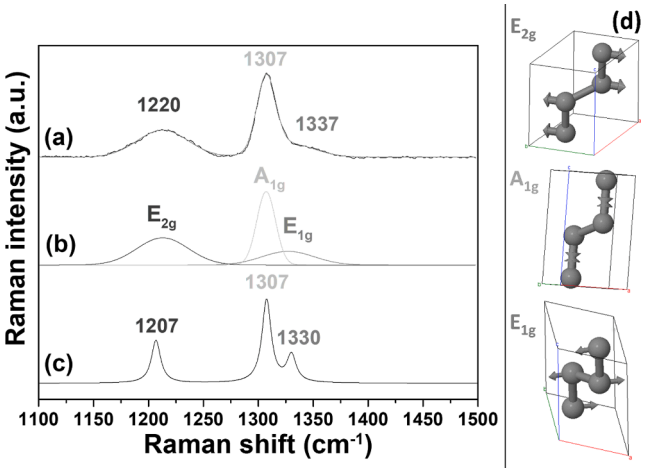

Fig. 4. (a) Experimental Raman spectrum of lonsdaleite (b) The active vibrational modes E_{1g}, A_{1g} and E_{2g} obtained via deconvolution of the Raman experimental spectrum, (c) Theoretical Raman spectrum of lonsdaleite with Gaussian line shape and a FWHM of 10 cm^{-1} and (d) The presentation of the Raman vibration modes of lonsdaleite.

Table 1
Raman shifts of 3C and 2H diamonds vibration bands.

Polytypes	a (Å)	c (Å)	Wavenumber (cm^{-1})		Experimental FWHM (cm^{-1})	Symmetry	Intensity (a. u.)
			Theoretical	Experimental			
3C diamond	3.5887	–	1332	1328–1331	4.9–7.3	F_{2g}	–
Lonsdaleite	2.5240	4.1999	1207	1220	37	E_{2g}	514
			1307	1307	18	A_{1g}	1000
			1330	1337	52	E_{1g}	326

Table 2
Calculate elastic constant *Cij*, bulk modulus *B*, shear modulus G and young modulus E (in GPa) of 3C- and 2H- diamond.

Structures	Space group	Methods	*B*	*G*	*E*	C_{11}	C_{12}	C_{13}	C_{33}	C_{44}	C_{66}	Reference
3C-Diamond	*F*-43*m*	Theoretical	453	517		1079	140	–	–	577	–	[55]
			432		1110	1047	124	–	–	559	–	[50]
			441			1087	116	–	–	575	–	This work
		Experimental	442	535	1143	1079	124	–	–	578	–	[56]
2H-Diamond	$P6_3mc$	Theoretical	432	523	1118	1182	95	12	1289	457	543	[50]
			466	541	1170	1244	118	24	1374	468	536	[57]
			460	542	1168	1207	94	12	1311	476	556	This work

hexagonal structure of diamond. The C_{33} value is superior to C_{11} value. This show that the compressibility along the *ab*-plane is more pronounced than along the *c*-axis, reducing the system more anisotropic.

3.4. Electronic properties of diamond

The cubic diamond face-centered cubic Bravais lattice with two atoms in the basis, while the hexagonal diamond has four per cell. As a result, the hexagonal structure has twice as many bands compared to the cubic structure at the K- point of the reconstructed cell in the Brillouin zone.

The electronic band structure of lonsdaleite by DFT calculation is presented in Fig. 5. The valence band is completely occupied, and the conduction band is fully empty. Therefore, the 2H-diamond polytype belongs to the group-IV semiconductors. Fig. 4 shows that the 2H-diamond is an indirect semiconductor since the wave vector at which the valence band is a maximum (Γ, Gamma point) and does not coincide with the wave vector where the conduction band is a minimum along the *K* symmetry line. The results here indicate that the electronic properties of hexagonal diamond differ from cubic diamond. The hexagonal diamond indirect bandgap was found to be 0.5 eV lower than the cubic diamond. Indeed, the calculated indirect bandgap of lonsdaleite and cubic diamond at room temperature are 5.2 eV and 5.7 eV, respectively. The calculated band gap of cubic diamond is closer to experimental value (5.47 eV) obtained by Koizumi [58].

4. Conclusion

In this study, we report the first occurrence of lonsdaleite polytype as mineral in surficial formed siliceous rock at P-T conditions of lower mantle which has undergone serpentinization and weathering by following metamorphic transformation. The originality here comes from the fact that lonsdaleite has been first observed in meteorite-transformed rocks from the Meteor Crater (Canyon Diablo Meteorite, Arizona). During next decades the evidence of lonsdaleite were found from different impact craters (Popigai, Zapadnaya and others [47,49,59]).

The calculated indirect bandgap of lonsdaleite at room temperature is slightly lower than that of cubic diamond. Lonsdaleite has potentially superior mechanical properties, such as hardness and rigidity, which exceed those of cubic diamond. However, these superior properties of lonsdaleite have never been proven experimentally due to the inability of synthesizing lonsdaleite in pure phase.

Finally, our results suggest further in-depth studies on the laterite formed on serpentinized peridotites.

CRediT authorship contribution statement

Yassine El Mendili: Conceptualization, Methodology, Software, Validation, Formal analysis, Investigation, Resources, Writing – original draft, Writing – review & editing, Visualization. **Beate Orberger:** Conceptualization, Methodology, Validation, Formal analysis,

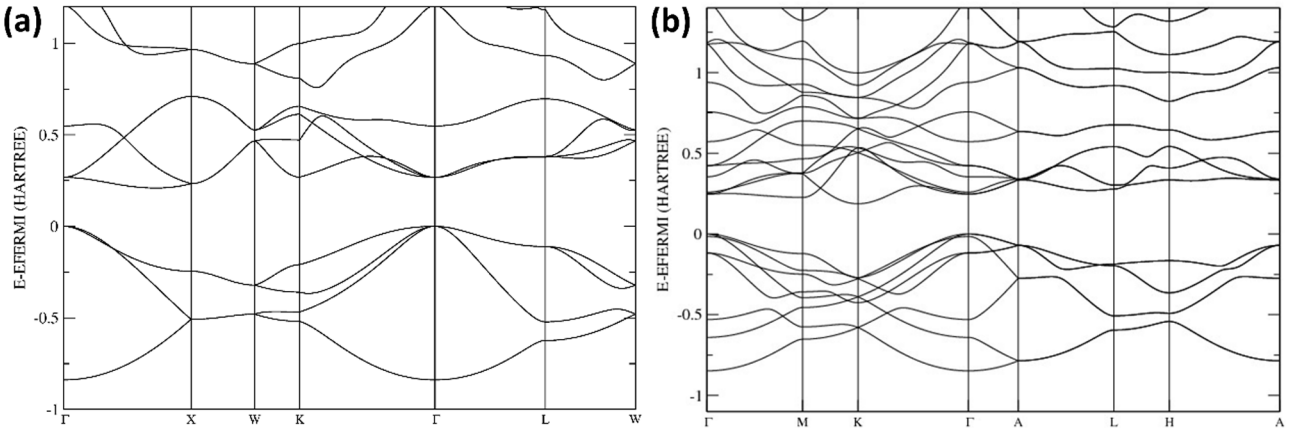

Fig. 5. Calculated electronic band structure of (a): cubic diamond and (b): lonsdaleite.

Investigation, Resources. **Daniel Chateigner:** Conceptualization, Methodology, Software, Validation, Formal analysis, Investigation, Resources, Writing – original draft, Writing – review & editing, Visualization. **Jean-François Bardeau:** Methodology, Software, Formal analysis, Investigation, Writing – original draft, Writing – review & editing, Visualization. **Stéphanie Gascoin:** Conceptualization, Methodology, Software, Formal analysis, Investigation, Writing – original draft, Writing – review & editing, Visualization. **Sébastien Petit:** Methodology, Software, Investigation.

Declaration of Competing Interest

The authors declare that they have no known competing financial interests or personal relationships that could have appeared to influence the work reported in this paper.

Acknowledgment

We thank the SLN for providing the sample material, and the BRGM staff for preparing the samples.

Funding Sources

We thank the European Commission for having sponsored this study in the frame of the SOLSA project (H2020 program) [Grant Number: SC5-11d-689868]. The DFT calculation work was done with the support of the French national computer center IDRIS under project n°081842 and the regional computer center CRIANN under project n°2007013.

References

[1] C. Frondel, U.B. Marvin, Lonsdaleite, a new hexagonal polymorph of diamond, Nature 214 (1967) 587–589, https://doi.org/10.1038/214587a0.
[2] Clifford Frondel, U.B. Marvin, Lonsdaleite, a hexagonal polymorph of diamond, Am. Mi. 214 (5088) (1967) 587–589.
[3] F. Langenhorst, M. Campione, Ideal and real structures of different forms of carbon, with some remarks on their geological significance, J. Geolog. Soc. 176 (2) (2019) 337–347, https://doi.org/10.1144/jgs2018-056.
[4] E.A. Belenkov, V.A. Greshnyakov, Structure, properties, and possible mechanism of formation of diamond-like phases, Phys. Solid State 58 (2016) 2145–2154, https://doi.org/10.1134/S1063783416100073.
[5] J.A. Baimova, L.K. Rysaeva, A.I. Rudskoy, Deformation behavior of graphite to the diamond-like phase, Diam. Relat. Mater. 81 (2018) 154–160, https://doi.org/10.1016/j.diamond.2017.12.001.
[6] V.A. Greshnyakov, E.A. Belenkov, Calculation of the physicochemical characteristics of a new orthorhombic form of diamond, Inorg. Mater. 54 (2) (2018) 111–116, https://doi.org/10.1134/S0020168518020061.
[7] Z. Pan, H. Sun, Y. Zhang, C. Chen, Harder than diamond: superior indentation strength of wurtzite BN and lonsdaleite, Phys. Rev. Let. 102 (2009) 055503, https://doi.org/10.1103/PhysRevLett.102.055503.
[8] F.P. Bundy, J.S. Kasper, Hexagonal diamond-a new form of carbon, Chem. Phys. 46 (9) (1967) 3437–3446, https://doi.org/10.1063/1.1841236.
[9] S.K. Simakov, V.T. Dubinchuk, M.P. Novikov, I.A. Drozdova, Formation of diamond and diamond-type phases from the carbon-bearing fluid at PT parameters corresponding to processes in the Earth's crust, Dokl. Earth Sci. 421 (1) (2008) 835–837, https://doi.org/10.1134/S1028334X08050280.
[10] P. Nemeth, L.A.J. Garvie, T. Aoki, N. Dubrovinskaia, L. Dubrovinsky, P.R. Buseck, Lonsdaleite is faulted and twinned cubic diamond and does not exist as a discrete material, Nature Commun. 5 (2014) 5447, https://doi.org/10.1038/ncomms6447.
[11] F.V. Kaminskii, G.K. Blinova, E.M. Galimov, G.A. Gurkina, Y.A. Klyuev, L. A. Kodina, V.I. Koptil, V.F. Krivonos, L.N. Frolova, A.Y. Khrenov, Polycrystalline aggregates of diamond with lonsdaleite from Yakutian [Sakhan] placers, Mineral. Zhurnal. 7 (1985) 27–36.
[12] I. Israde-Alcántara, J.L. Bischoff, G. Domínguez-Vázquez, H.-C. Li, P.S. DeCarli, T. E. Bunch, J.H. Wittke, J.C. Weaver, R.B. Firestone, A. West, J.P. Kennett, C. Mercer, S. Xie, E.K. Richman, C.R. Kinzie, W.S. Wolbach, Evidence from central Mexico supporting the Younger Dryas extraterrestrial impact hypothesis, Proc. Natl. Acad. Sci. 109 (13) (2012), https://doi.org/10.1073/pnas.1110614109.
[13] T.L. Daulton, N. Pinter, A.C. Scott, No evidence of nanodiamonds in Younger-Dryas sediments to support an impact event, Proc. Natl. Acad. Sci. 107 (2010) (2010) 16043–16047, https://doi.org/10.1073/pnas.1003904107.
[14] T.L. Daulton, S. Amari, A.C. Scott, M. Hardiman, N. Pinter, R.S. Anderson, Comprehensive analysis of nanodiamond evidence relating to the Younger Dryas Impact Hypothesis, J. Quat.. Sci. 32 (1) (2017) 7–34, https://doi.org/10.1002/jqs.2892.
[15] D. Kraus, A. Ravasio, M. Gauthier, D.O. Gericke, J. Vorberger, S. Frydrych, J. Helfrich, L.B. Fletcher, G. Schaumann, B. Nagler, B. Barbrel, B. Bachmann, E. J. Gamboa, S. Göde, E. Granados, G. Gregori, H.J. Lee, P. Neumayer, W. Schumaker, T. Döppner, R.W. Falcone, S.H. Glenzer, M. Roth, Nanosecond formation of diamond and lonsdaleite by shock compression of graphite, Nat. Commun. 7 (2016) 10970, https://doi.org/10.1038/ncomms10970.
[16] V.T. Dubinchuk, S.K. Simakov, V.A. Pechnikov, Lonsdaleite in diamond-bearing metamorphic rocks of the Kokchetav massif, Dokl. Earth. Sci. 430 (1) (2010) 40–42, https://doi.org/10.1134/S1028334X10010083.
[17] Y. Nakamuta, S. Toh, Transformation of graphite to lonsdaleite and diamond in the Goalpara ureilite directly observed by TEM, Am. Mineral. 98 (4) (2013) 574–581, https://doi.org/10.2138/am.2013.4341.
[18] R.E. Hanneman, H.M. Strong, F.P. Bundy, Hexagonal diamonds in meteorites: implications, Science 155 (1967) 995–997, https://doi.org/10.1126/science.155.3765.995.
[19] F.P. Bundy, J.S. Kasper, Hexagonal diamond - a new form of carbon, J. Chem. Phys. 46 (9) (1967) 3437–3446, https://doi.org/10.1063/1.1841236.
[20] Sabri Ergun, L.E. Alexander, Crystalline forms of carbon: a possible hexagonal polymorph of diamond, Nature 195 (4843) (1962) 765–767, https://doi.org/10.1038/195765a0.
[21] Y. El Mendili, B. Orberger, D. Chateigner, J.-F. Bardeau, S. Gascoin, S. Petit, O. Perez, F. Khadraoui, Insight into the structural, elastic and electronic properties of a new orthorhombic 6O-SiC polytype, Sci. Rep. 10 (2020) 7562, https://doi.org/10.1038/s41598-020-64415-4.
[22] Y. El Mendili, B. Orberger, D. Chateigner, J.-F. Bardeau, S. Gascoin, S. Petit, O. Perez, Occurrence of SiC and diamond polytypes, chromite and uranophane in breccia from nickel laterites (New Caledonia): combined analyses, Minerals 12 (2) (2022) 196, https://doi.org/10.3390/min12020196.
[23] N. Pujol-Solà, J.A. Proenza, A. Garcia-Casco, J.M. González-Jiménez, A. Andreazini, J.C. Melgarejo, et al., An alterna-514 tive scenario on the origin of ultra-high pressure (UHP) and super-reduced (SuR) minerals in ophiolitic chromitites: a case 515 Study from the mercedita deposit (Eastern Cuba), Minerals 8 (10) (2018) 433, https://doi.org/10.3390/min8100433.
[24] C. Duée, B. Orberger, N. Maubec, V. Laperche, L. Capar, A. Bourguignon, X. Bourrat, Y. El Mendili, D. Chateigner, S. Gascoin, M. Le Guen, C. Rodriguez, F. Trotet, M. Kadar, K. Devaux, M. Ollier, H. Pillière, T. Lefèvre, D. Harang, F. Eijkelkamp, H. Nolte, P. Koert, Impact of heterogeneities and surface roughness on pXRF, pIR, XRD and Raman analyses: challenges for on-line, real-time combined mineralogical and chemical analyses on drill cores and implication for "high speed" Ni-laterite exploration, J. Geochem. Explor. 198 (2019) 1–17, https://doi.org/10.1016/j.gexplo.2018.12.010.
[25] Y. El Mendili, D. Chateigner, B. Orberger, S. Gascoin, J.-F. Bardeau, S. Petit, et al., Combined XRF, XRD, SEM-EDS, and Raman analyses on Serpentinized Harzburgite (Nickel Laterite Mine, New Caledonia): implications for exploration and geometallurgy, ACS Earth. Space. Chem. 3 (2019) 2237–2249, https://doi.org/10.1021/acsearthspacechem.9b00014.
[26] R.B. Trumbull, J.-S. Yang, P.T. Robinson, S. Di Pierro, T. Vennemann, M. Wiedenbeck, The carbon isotope composition of natural SiC (moissanite) from the Earth's mantle. New discoveries from ophiolites, Lithos 113 (3-4) (2009) 612–620, https://doi.org/10.1016/j.lithos.2009.06.033.
[27] L. Bailly, J. P. Ambrosi, J. Barbarand, A. Beauvais, D. Cluzel, Nickel - Typologie des latérites de Nouvelle-Calédonie. Gisements de nickel latéritique, volume II. [Rapport de recherche] tome Nickel et Technologie, CNRT "Nickel et son environnement". ird-01938833, 2014, pp. 1–448.
[28] J.J. Trescases, The lateritic nickel-ore deposits, in: H. Paquet, N. Clauer (Eds.), Soils and Sediments Mineralogy and Geochemistry, Springer, Berlin, 1997, pp. 125–138.
[29] K.D. Litasov, H. Kagi, T.B. Bekker, Enigmatic super-reduced phases in corundum from natural rocks: possible contamination from artificial abrasive materials or metallurgical slags, Lithos 340–341 (2019) 181–190, https://doi.org/10.1016/j.lithos.2019.05.013.
[30] K.D. Litasov, H. Kagi, S.A. Voropaev, T. Hirata, H. Ohfuji, H. Ishibashi, Y. Makino, T.B. Bekker, V.S. Sevastyanov, V.P. Afanasiev, N.P. Pokhilenko, Comparison of enigmatic diamonds from the Tolbachik arc volcano (Kamchatka)and Tibetan ophiolites: assessing the role of contamination by synthetic materials, Gondwana Res. 75 (2019) 16–27, https://doi.org/10.1016/j.gr.2019.04.007.
[31] K.D. Litasov, H. Kagi, T.B. Bekker, Y. Makino, T. Hirata, V.V. Brazhkin, Why Tolbachik diamonds cannot be natural, Am. Mineral. 106 (2021) 44–53, https://doi.org/10.2138/am-2020-7562.
[32] R. Dovesi, R. Orlando, A. Erba, C.M. Zicovich-Wilson, B. Civalleri, S. Casassa, L. Maschio, M.D. Ferrabone, M. La Pierre, P. D'Arco, Y. Noel, M. Causa, M. Rerat, B. Kirtman, CRYSTAL14: a program for the ab initio investigation of crystalline solids, Int. J. Quantum Chem. 114 (2014) 1287–1317, https://doi.org/10.1002/qua.24658.
[33] C. Gatti, V.R. Saunders, C. Roetti, Crystal field effects on the topological properties of the electron density in molecular crystals: the case of urea, J. Chem. Phys. 101 (12) (1994) 10686–10696, https://doi.org/10.1063/1.467882.
[34] F. Pascale, C.M. Zicovich-Wilson, F. López Gejo, B. Civalleri, R. Orlando, R. Dovesi, The calculation of the vibrational frequencies of crystalline compounds and its implementation in the CRYSTAL code, J. Comput. Chem. 25 (6) (2004) 888–897, https://doi.org/10.1002/jcc.20019.
[35] C.M. Zicovich-Wilson, F. Pascale, C. Roetti, V.R. Saunders, R. Orlando, R. Dovesi, Calculation of the vibration frequencies of α-quartz: the effect of Hamiltonian and basis set, J. Comput. Chem. 25 (2004) 1873–1881, https://doi.org/10.1002/jcc.20120.
[36] L. Maschio, B. Kirtman, M. Rérat, R. Orlando, R. Dovesi, Ab initio analytical Raman intensities for periodic systems through a coupled perturbed Hartree-Fock/Kohn-Sham method in an atomic orbital basis. I. Theory, J. Chem. Phys. 139 (16) (2013) 164101, https://doi.org/10.1063/1.4824442.

[37] L. Maschio, B. Kirtman, M. Rérat, R. Orlando, R. Dovesi, Ab initio analytical Raman intensities for periodic systems through a coupled perturbed Hartree-Fock/Kohn-Sham method in an atomic orbital basis. II. Validation and comparison with experiments, J. Chem. Phys. 139 (16) (2013) 164102, https://doi.org/10.1063/1.4824443.
[38] M. Ferrero, M. Rérat, R. Orlando, R. Dovesi, The calculation of static polarizabilities of 1–3D periodic compounds. The implementation in the crystal code, J. Comput. Chem. 29 (9) (2008) 1450–1459, https://doi.org/10.1002/jcc.20905.
[39] M. Ferrero, M. Rérat, R. Orlando, R. Dovesi, Coupled perturbed Hartree-Fock for periodic systems: the role of symmetry and related computational aspects, J. Chem. Phys. 128 (1) (2008) 014110, https://doi.org/10.1063/1.2817596.
[40] K.E. Spear, A.W. Phelps, W.B. White, Diamond and diamond-like materials, J. Mater. Res. 5 (1990) 2277–2285, https://doi.org/10.1557/JMR.1990.2277.
[41] P. Németh, L.A.J. Garvie, T. Aoki, N. Dubrovinskaia, L. Dubrovinsky, P.R. Buseck, Lonsdaleite is faulted and twinned cubic diamond and does not exist as a discrete material, Nat. Comm. 5 (2014) 5447, https://doi.org/10.1038/ncomms6447.
[42] D. Kraus, A. Ravasio, M. Gauthier, D.O. Gericke, J. Vorberger, S. Frydrych, J. Helfrich, L.B. Fletcher, G. Schaumann, B. Nagler, B. Barbrel, B. Bachmann, E. J. Gamboa, S. Göde, E. Granados, G. Gregori, H.J. Lee, P. Neumayer, W. Schumaker, T. Döppner, R.W. Falcone, S.H. Glenzer, M. Roth, Nanosecond formation of diamond and lonsdaleite by shock compression of graphite, Nat. Commun. 7 (1) (2016), https://doi.org/10.1038/ncomms10970.
[43] D.C. Smith, G. Godard, UV and VIS Raman spectra of natural lonsdaleites: towards a recognised standard, Spectrochimica. Acta. Part. A 73 (3) (2009) 428–435, https://doi.org/10.1016/j.saa.2008.10.025.
[44] S.J. Turneaure, S.M. Sharma, T.J. Volz, J.M. Winey, Y.M. Gupta, Transformation of shock-compressed graphite to hexagonal diamond in nanoseconds, Sci. Adv. 3 (2017) eaao3561, https://doi.org/10.1126/sciadv.aao3561.
[45] M. Nishitani-Gamo, I. Sakaguchi, K.P. Loh, H. Kanda, T. Ando, Confocal Raman spectroscopic observation of hexagonal diamond formation from dissolved carbon in nickel under chemical vapor deposition conditions, Appl. Phys. Lett. 73 (6) (1998) 765–767, https://doi.org/10.1063/1.121994.
[46] B.R. Wu, Structural and vibrational properties of the 6H diamond: first-principles study, Diamond. Relat. Mater 16 (1) (2007) 21–28, https://doi.org/10.1016/j.diamond.2006.03.013.
[47] S.V. Goryainov, A.Y. Likhacheva, S.V. Rashchenko, A.S. Shubin, V.P. Afanas'ev, N. P. Pokhilenko, Raman identification of lonsdaleite in Popigai impactites, J. Raman Spectrosc. 45 (4) (2014) 305–313, https://doi.org/10.1002/jrs.4457.
[48] V.P. Afanas'ev, K.D. Litasov, S.V. Goryainov, V.V. Kovalevskii, Raman spectroscopy of nanopolycrystalline diamond produced from shungite at 15 GPa and 1600°C, JETP Lett. 111 (4) (2020) 218–224, https://doi.org/10.1134/S0021364020040050.
[49] N.N. Ovsyuk, S.V. Goryainov, A.Y. Likhacheva, Raman scattering of impact diamonds, Diam. Related Mater. 91 (2019) 207–212, https://doi.org/10.1016/j.diamond.2018.11.017.
[50] Y. Wang, Q. Zeng, X. Du, Y. Gao, B. Yin, The structural, mechanical and electronic properties of novel superhard carbon allotropes: *ab initio* study, Mater. Today Commun. 29 (102980) (2021) 1–7, https://doi.org/10.1016/j.mtcomm.2021.102980.
[51] M. Yoshikawa, Y. Mori, H. Obata, M. Maegawa, G. Katagiri, H. Ishida, A. Ishitani, Raman scattering from nanometer-sized diamond, Appl. Phys. Lett. 67 (5) (1995) 694–696, https://doi.org/10.1063/1.115206.
[52] Z. Sun, J.R. Shi, B.K. Tay, S.P. Lau, UV Raman characteristics of nanocrystalline diamond films with different grain size, Diamond Relat. Mater. 9 (12) (2000) 1979–1983, https://doi.org/10.1016/S0925-9635(00)00349-6.
[53] N.V. Surovtsev, I.N. Kupriyanov, Temperature dependence of the Raman line width in diamond: revisited, J. Raman Spectrosc. 46 (1) (2015) 171–176, https://doi.org/10.1002/jrs.4604.
[54] V.N. Denisov, B.N. Mavrin, N.R. Serebryanaya, G.A. Dubitsky, V.V. Aksenenkov, A. N. Kirichenko, N.V. Kuzmin, B.A. Kulnitskiy, I.A. Perezhogin, V.D. Blank, First-principles, UV Raman, X-ray diffraction and TEM study of the structure and lattice dynamics of the diamond–lonsdaleite system, Diamond. Relat. Mater. 20 (7) (2011) 951–953, https://doi.org/10.1016/j.diamond.2011.05.013.
[55] M. Núñez Valdez, K. Umemoto, R.M. Wentzcovitch, Elasticity of diamond at high pressures and temperatures, Appl. Phys. Lett. 101 (17) (2012) 171902, https://doi.org/10.1063/1.4754548.
[56] H.J. McSkimin, P. Andreatch, Elastic moduli of diamond as a function of pressure and temperature, J. Appl. Phys. 43 (7) (1972) 2944–2948, https://doi.org/10.1063/1.1661636.
[57] T.A. Ivanova, B.N. Mavrin, First-principle study of structural and mechanical properties of hexagonal polytypes of diamond, Cryst. Rep. 60 (2) (2015) 257–262, https://doi.org/10.1134/S1063774515020108.
[58] Koizumi, S. Thin-Film Diamond I, Semiconductors and Semimetals, Vol. 76 (eds C. E. Nebel and I. Ristein), Elsevier Academic, Amsterdam, 2003.
[59] V.L. Masaitis, Popigai crater: origin and distribution of diamond-bearing impactites, Meteorit. Planet. Sci. 33 (2) (1998) 349–359, https://doi.org/10.1111/j.1945-5100.1998.tb01639.x.